PV module degradation in the field and in the lab - how does it fit together?

Cornelia Peike[1], Stephan Hoffmann[1], Ines Dürr[1], Karl-Anders Weiß[1], Nicolas Bogdanski[2], Michael Köhl[1]
[1]Fraunhofer Institute for Solar Energy Systems (ISE), Heidenhofstraße 2, D-79110 Freiburg, Germany
[2]TÜV Rheinland Group, Am Grauen Stein, 51105 Cologne, Germany

ABSTRACT:
To design realistic and quick accelerated aging tests, the comparison between the degradation mechanisms induced by outdoor exposure and by accelerated aging tests is indispensable. Various accelerated aging tests, i.e. heat aging, UV aging, damp-heat aging and combined UV / damp-heat aging, were performed on full-size PV modules from different PV module manufacturers. The climate-dependence of the degradation was investigated on identical PV modules which have been exposed in different extreme climates for up to six years. A comprehensive degradation analysis was performed, i.e. by means of power measurements, electroluminescence imaging and Raman spectroscopy. The electrical characterization showed a high stability of all investigated modules.

Keywords: Ethylene-vinyl acetate, degradation, non-destructive investigation, Raman Spectroscopy

1 INTRODUCTION

Accelerated aging tests are a major tool for PV module degradation analysis. Those tests are supposed to simulate the conditions a PV module is subjected to during its service life, only in a very short period of time. The design of the tests is very difficult, since a multitude of external and internal factors affect the exposed module. Those factors are, among other things, various different degradation mechanisms within the modules, such as encapsulation degradation, cell degradation or back-sheet delamination [1, 2, 3, 4, 5, 6]. Especially the degradation of the encapsulation material is highly dependent on the external factors, which are provided by the climate around the PV module [7, 8].

The aim of this work was to link accelerated aging tests to outdoor exposure tests. Therefore, the impact of different stress factors on the degradation of the encapsulation material in PV modules, which is often the weakest link, was investigated. Spatially-resolved Raman spectroscopic measurements were performed across selected cells of the modules, chosen on the basis of electroluminescence images, before and after aging.

To gain a deeper understanding of the impact of different stress factors on the encapsulation material, various accelerated aging tests, i.e. heat aging, UV aging, damp-heat aging and combined UV / damp-heat aging, have been performed on full-size PV modules from different PV module manufacturers. Spatially-resolved measurements across silicon cells were supposed to give information about the induced degradation patterns.

The climate-dependence of the encapsulation degradation was investigated on identical PV modules which have been exposed in different climates for up to six years, i.e. a moderate, a mountain, an arid and a tropic climate.

Due to the need for analytical methods which allow non-destructive, spatially-resolved measurements, Raman probe spectroscopy was chosen, which has been described as a method for polymer degradation characterization in PV modules, previously. The intensity of the detected fluorescence, which is caused by fluorophoric species within EVA [9] has been taken as a measure for the degree of polymer aging [10].

2 MATERIALS AND TECHNIQUES

2.1 Samples

The full-size PV modules which will be studied in chapter 6.3 were crystalline Si-PV modules from seven German manufacturers (S1 - S7). Sizes varied between 680 to 1000 (width) and 1466 to 2000 mm (height). All modules had a similar design, consisting of solar-glass glazing, fast-cure EVA encapsulation, poly- or mono-crystalline Si-cells, a TPT back-sheet, an aluminum frame and a junction box. The specific materials used are given in **Table 1**.

Table 1: The investigated additive compositions.

Type	Front side material	Encapsulation	Rear side material
S1	solar glass	EVA	TPT (170 μm)
S2	solar glass with Ce	EVA	TPT (290 μm)
S3	solar glass	EVA	TPT (350 μm)
S4	solar glass	EVA	TPE (275 μm)
S5	solar glass	EVA	TPT (290 μm)
S6	solar glass	EVA	TPT (290 μm)
S7	solar glass	EVA	TPT (170 μm)

TPT – Tedlar®/poly ethylene terephthalate/Tedlar®
TPE – Tedlar®/polyethylene terephthalate/polyethylene

The PV modules of manufacturer S2 were the only ones which had a solar glass which contained Cerium as UV absorber. All EVA encapsulants were PV specific foils with a vinyl acetate content of about 33%. The thickness of the TPT rear side material varied between 170 µm (S1 and S7) and 350 µm. Those thickness variations were due to PET core layers of different thicknesses. Therefore, the permeation properties of the different back-sheet materials vary for the different materials. All manufacturers, except for S4, used poly-crystalline silicon cells.

2.2 Aging tests

The damp-heat aging test (DH) was conducted according to IEC61215 (85 RH% at 85°C) for up to 4000h. An overview of the aging tests and conditions is given in Table 2.

Table 2: The accelerated aging conditions.

Aging test	Abbreviation	T_{av} [°C]	RH_{av} [%]	$H_c[kWh/m^2]$	$t_{ges}[h]$
No aging	ref	-	-	-	-
Heat aging	H	90	< 5%	0	2000
UV aging	UV	60	< 5%	240	1300
UV/ damp-heat aging	UV/DH	60	60	108	950
Damp heat aging	DH	85	85	0	4000

Additional to the accelerated aging tests, the seven different module types were exposed outdoors in four different climates for up to three years as shown in Table 3. The chosen exposition sites were a mountain climate at mount Zugspitze in Germany, a moderate climate in Cologne in Germany, an arid climate in the Negev desert in Israel and a tropic climate in Serpong, Indonesia. Initial characterizations of the electrical and chemical properties of the modules were carried out at the Fraunhofer ISE in Germany. Afterwards, the modules were shipped (Indonesia and Israel) or transported (Cologne and Zugspitze) to their respective exposition sites. The modules were mounted on free-standing racks in adequate mounting angles.

Table 3: The outdoor aging conditions [12].

Exposition site	Climate	T_{av}	T_{max}	T_{min}	RH_{av}	G
			[°C]		[%]	[kWh/am^2]
Negev, Israel	arid	18	39	-5	69	2269
Serpong, Indonesia	tropic	27	37	19	79	1626
Cologne, Germany	moderate	12	36	-14	76	1184
Zugspitze, Germany	mountain	0	21	-25	78	1169

T_{av} - average ambient temperature within exposition period
T_{max}/T_{min} - maximum and minimum ambient temperatures within the exposition period
RH_{av} - average relative humidity within exposition period
G - annual irradiation within exposition period

2.3 Analytics

The initial characterizations as well as the measurements after three years of outdoor exposure were carried out at the Fraunhofer ISE. Electroluminescence imaging was performed with a Greateyes GE 1024 256 NIR camera. IV curves were measured at Fraunhofer ISE CalLab PV Modules with a h.a.l.m. cetisPV XF2M A080664 according to IEC 60904-1 and IEC 60904-3.
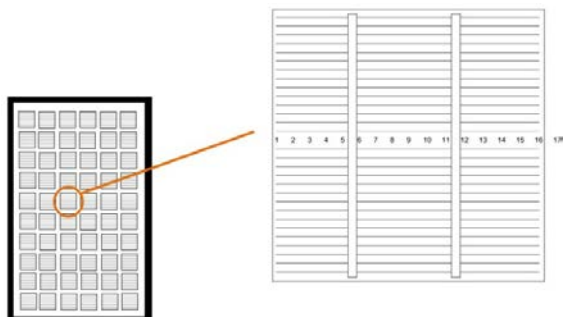

Figure 1: The Raman spectroscopic measurements were carried out using equidistant measurement points, horizontal across the cell.

Raman Measurements were carried out on commercial PV modules using a WiTec Alpha 500 Raman Microscope with a remote Raman probe attachment. The 532 nm line of a frequency doubled Nd:YAG laser with an excitation power of 16,6 mW was used as excitation source. The InPhotonics

fiber optic Raman probe RPB532, constructed with a 105 µm excitation fiber and 200 µm collection fiber, was used. A thermoelectrically cooled CCD was employed for detection. The measurement set up and the spatial resolution are described elsewhere [11]. Measurements were carried out at equidistant points across the entire cell in order to investigate the influence of the location relative to the cell on the degradation behavior of the encapsulation. All measurements were carried out with an integration time of 0.5 sec in the encapsulation between the glazing and the cell and an average of twenty single measurements was calculated for each spectrum.

3 RESULTS

3.1 Power measurements

The power output measurements of the aged modules, shown in Table 4, revealed an almost negligible impact of the heat aging (2000 h), the UV (240kWh/m^2) aging and the combined UV/DH aging (950 h, 108 kWh/m^2). In contrast to that, the damp-heat aging test (4000 h) induced significant power losses in all modules. DH-induced power losses ranged between -38.7 and -82.3%.

Table 4: Changes of the performance of the PV modules after three years of indoor aging relative to the initial value.

Aging test	S1	S2	S3	S4	S5	S6	S7
				P[%]			
Heat aging	-0.1	-2.8	-1.2	±0	+ 0.4	-0.3	-2.1
Damp-heat aging	-38.7	-82.3	-77.3	-48.6	-73.4	-62.3	-61.6
UV aging	-2.9	-3.8	-	-2.1	-1.4	-0.9	-0.6
UV/ damp-heat aging	-5.6	-3.2	-	-1.4	-0.1	-0.1	-0.4

The influence of the three years of outdoor aging in the respective climates appeared to have very little impact on the power output of the modules (Table 5). Except for the mountain aged modules S7 and S6, all modules showed only power variations between 0.1 and 1.7%. The mountain exposed module S5 even showed a slight gain in power output of 1.3% after the three years. These variations are within the measurement uncertainties of about 2%. The only module with a rather high power output variation was the mountain aged module S7 which displayed a power decrease of 6.6%, exhibited severe cell cracking and those cell cracks resulted in isolated cell parts which caused a reduced power output.

Table 5: Changes of the performance of the PV modules after three years of outdoor aging relative to the initial value.

Aging test	S1	S2	S3	S4	S5	S6	S7
				P[%]			
Moderate	-0.6	-1.8	-0.1	-0.8	-0.5	-0.9	+1.7
Mountain	-1.1	-0.8	-6.2	-1.1	+1.3	-4.7	-6.6
Arid	-0.8	-2.2	-0.1	-0.6	-1.1	-0.1	-0.1
Tropic	-1.3	-3.2	-0.3	-1.5	-0.1	-0.1	-1.0

3.2 Comparison indoor/ outdoor aging

Exemplarily, the Raman Spectra measured in the middle of the cell of the modules of type S7 after the different accelerated and outdoor aging tests are shown in Figure 2. The accelerated aging test (a) as well as the outdoor exposition in different climates (b) resulted in very different EVA Raman spectra. The UV and the UV/DH aged modules showed spectra with an intense fluorescence and no detectable EVA peaks. These spectra appeared to be similar to that after outdoor exposure in an arid climate for three years. The fine structure of all the spectra is similar up to relative wavenumber of about 1300 cm^{-1}.
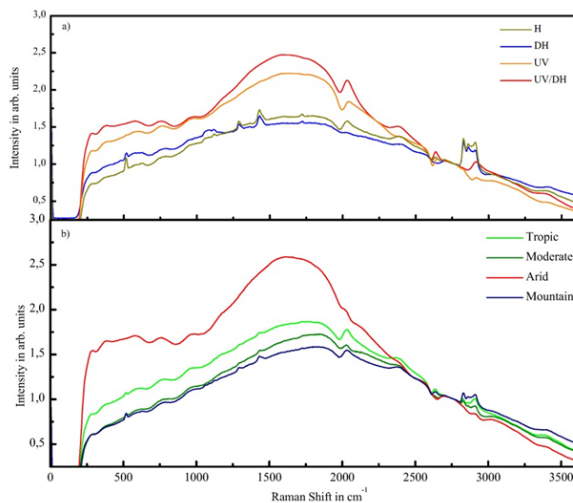
Figure 2: Comparison of Raman spectra, measured in the center of a cell of module S7, after accelerated aging tests (a) and after three years of outdoor exposure (b).

In order to evaluate the differences between the degradational changes which were induced by the different aging tests in a semi-quantitative manner, also the fluorescence intensities are compared. This way, the spatial dependence of the impact of the different aging tests can be elucidated. The comparison of the distribution of fluorescence intensities, induced by accelerated indoor aging as well as by outdoor aging, are shown in Figure 3.

For the type S5 modules the damp-heat aging caused a relatively high fluorescence along a five centimeters broad area at the edges of the cell. The fluorescence in the center of the cell is significantly lower and homogeneously distributed. The heat aging induced little fluorescence with homogeneous distribution across the whole cell. UV and UV/DH aging resulted in the highest fluorescence intensities and fluorescence intensities were, especially after UV aging, slightly lower at the edges of the cell.

All outdoor exposures induced a similar fluorescence intensity distribution for the S5-type modules with high fluorescence in the center of the cells and lower values at the edges. Highest intensity values were reached after aging in an arid and a tropic climate, followed by the mountain and the moderate climate. Those different intensity values show that the degree of aging is highly dependent on the exposition site as a result of differences in irradiation, temperature and humidity. The arid climate exhibits the highest maximum temperatures, the highest UV irradiation as well as lowest relative humidity values of all exposition sites whereas in the tropic climate, the

highest average temperature and high UV-irradiation. This explains the highest fluorescence values after aging in an arid or tropic climate. Comparing the fluorescence intensity distributions induced by the accelerated aging tests to that after outdoor exposure, the S5-heat, S5-damp-heat and the S5-UV/DH fluorescence distributions are in no way comparable to either one of the outdoor aged S5 modules. The discrepancy between the fluorescence intensity distributions is the biggest for the damp-heat aged S5-module due to the inverse fluorescence distribution. Only the S5-UV module showed a similarity to the outdoor aging results, both in fluorescence distribution and in intensity, which was comparable to that after three years of outdoor aging in an arid or tropic climate.
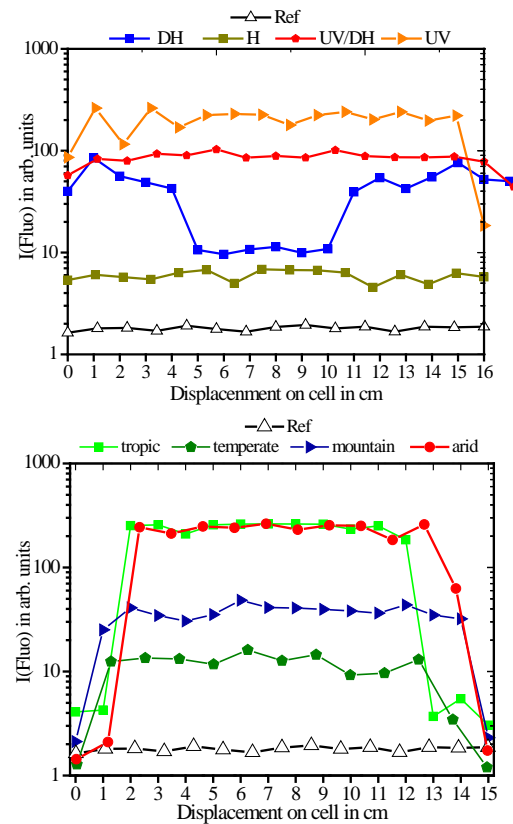

Figure 3: Comparison of the distribution of the fluorescence intensity across one cell, calculated from the Raman spectra, in modules of type S7 after outdoor and indoor aging.

After this fist aging period, modules were aged for three more years. Exemplarily, the results of the modules aged in a tropic climate are presented here.

Figure 5 shows the electroluminescence images as well as the distribution of the fluorescence intensity across the cells of the different modules after six years of outdoor aging in a tropic climate.

None of the cells showed cell cracks of other degradation patterns in the EL images. In contrast to that, the distribution of the fluorescence intensities appeared to be very different for the different types of modules. While the modules of types S6 and S7 displayed similar fluorescence distribution patterns, modules S2 and S4 showed much weaker fluorescence (S2) and a broader area of no fluorescence at the edges of the cells (S4).

Those phenomena can be explained by the different backsheet foil which is used for module S4 (TPE instead of TPT) and by the presence of Ce UV absorber in the front glass of module S4.
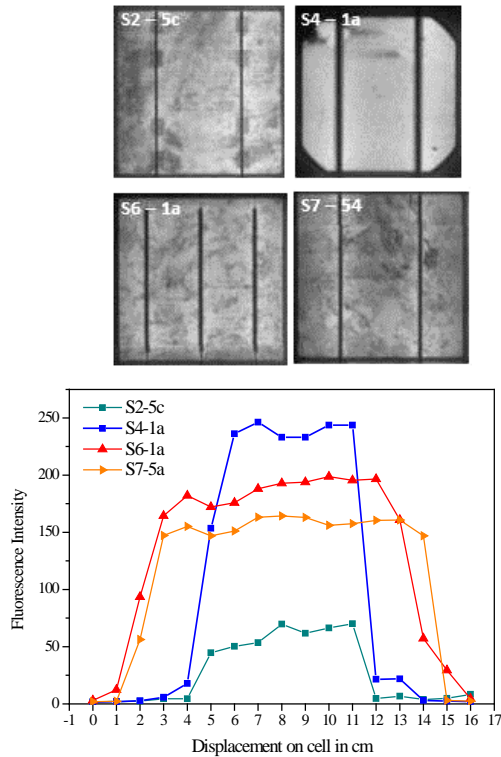

Figure 4: Top: Electroluminescence image of the measured cells of the different modules after six years of outdoor aging in a tropic climate. Bottom: Comparison of the distribution of the fluorescence intensity across the cells, calculated from the Raman spectra.

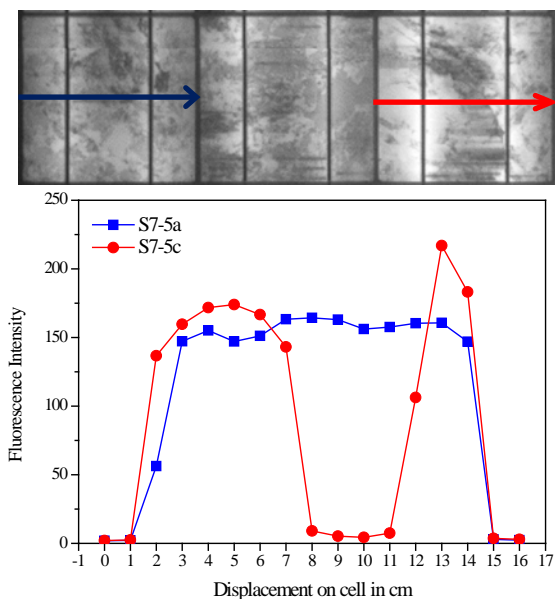A further interesting phenomenon can be found when comparing two cells in module S7 (Figure 5).

Figure 5: Top: Electroluminescence image of cells in a module type S7 after six years of outdoor aging in a tropic climate. Bottom: Distribution of the fluorescence intensity across two cells of the module, calculated from the Raman spectra.

One of those cells showed no crack (5a) and for the other cell (5c) a slight crack in the center of the cell could be observed, hardly visible in the EL image (Figure 5, top). While cell 5a showed a homogeneously distributed fluorescence across the central area of the cell, cell 5c displayed an abrupt decrease of the fluorescence intensity in the area of the slightly visible crack. This effect can by explained by altered diffusion conditions in the area of the cell crack which result in the photobleaching of the fluorophoric species. This way, it can be determined whether a certain "shadow" in an EL image is a cell crack or not.

4 Conclusion

The aim of this work was to link accelerated aging test results to those of outdoor exposure tests. Therefore, the impact of different stress factors on the degradation of the encapsulation material in PV modules was investigated. All outdoor aging tests, especially those in the tropic and the arid climates, resulted in similar fluorescence intensity patterns across the cell. Those tests resulted in high fluorescence intensities in the encapsulant above the center of the cells and decreasing values towards the edges of the cells. Modules which were subjected to outdoor aging in a moderate or mountain climate similarly to the other fluorescence distributions behaved but exhibited lower fluorescence intensities compared to arid and tropical climates after identical periods of time. Comparing the degradation patterns induced by the outdoor and indoor aging tests, the highest similarities between outdoor and indoor aging were found after indoor aging tests with UV irradiation, i.e. UV aging and combined UV/damp-heat. This finding indicates the photochemical degradation to be the driving force in fluorescence evolution.

5 REFERENCES

[1]   M.A. Quintana, D.L. King, T.J. McMahon, C.R. Osterwald, *Commonly observed Degradation in Field-Aged Photovoltaic Modules*, proc. IEEE, pp. 1436-1439 (2002).

[2]   E.E. van Dyk, J.B. Chamel, A.R. Gxasheka, *Investigation of delamination in an edge-difined film-def growth photovoltaic module*, Solar Energy Materials & Solar Cells, 88, pp. 403-411 (2005).

[3]   P. Sanchez-Friera, M. Piligougine, J. Peláez, J. Carretero, M. Sidrach de Cardona, *Analysis of degradation mechanisms of crystalline silicon PV modules after 12 years of operation in Southern Europe*, Prog. Photovol: Res. Appl., 19, pp. 658-666 (2011).

[4]   A. Paretta, M. Bombace, G. Graditi, R. Schioppo, *Optical degradation of long- term, field-aged c–Si photovoltaic modules*, Solar Energy Materials & Solar Cells 86, pp. 349–364 (2005).

[5]   C. Dechthummarong, B. Wiengmoon, D. Chenvidhya, C. Jivacate, K. Kirtikara, *Physical deterioration of*

encapsulation and electrical insulation properties of PV modules after long-term exposure in Thailand, Solar Energy Materials & Solar Cells 94 (9), pp.1437-1440 (2010).

[6] N.R. Wheeler, L.S. Bruckman, J. Ma, E. Wang, C. K. Wang, I. Chou, J. Sun, R.H. French, *Degradation pathway models for photovoltaics module lifetime performance*, proc. IEEE, (2013).

[7] P. Klemchuk, M. Ezrin, G. Lavigne, W. Holley, J. Galica, S. Agro, *Investigation of the degradation and stabilization of EVA-based encapsulant in field-aged solar energy modules*, Polymer Degradation and Stability, 55, pp. 347-365 (1997).

[8] N.S. Allen, M. Edge, M. Rodriguez, C.M. Liauw, E. Fontan, *Aspects of thermal oxidation, yellowing and stabilization of ethylene vinyl acetate copolymer*, Polymer Degradation and Stability, 71, pp.1-14, (2001).

[9] C.Peike, T. Kaltenbach, K.-A. Weiss, M. Köhl, *Non-destructive degradation analysis of encapsulants in PV modules by Raman Spectroscopy*, Solar Energy Materials & Solar Cells, vol.95, pp. 1686-1693 (2011).

[10] C. Peike, L. Purschke, K.-A. Weiss, M.D. Kempe, M. Köhl, *Towards the origin of photochemical EVA discoloration.,* proc. IEEE 39th. 2013.

[11] C. Peike, S. Hoffmann, M. Heck, T. Kaltenbach, K.-A. Weiß, M. Köhl, *Nondestructive Determination of Climate-Specific Degradation Patterns for Photovoltaic-Module Encapsulation*, Energy Technology, 2, 121–129 (2014).

[12] M. Koehl, M. Heck, S. Wiesmeier, J. Wirth, *Modeling of the nominal operating cell temperature based on outdoor weathering,* Solar Energy Materials & Solar Cells, 95 (7), 1638-1646 (2011).